

# Increased renal calcium and magnesium transporter abundance in streptozotocin-induced diabetes mellitus

C-T Lee<sup>1,2</sup>, Y-HH Lien<sup>3</sup>, L-W Lai<sup>3</sup>, J-B Chen<sup>1</sup>, C-R Lin<sup>4</sup> and H-C Chen<sup>2</sup>

<sup>1</sup>Division of Nephrology, Department of Medicine, Chang-Gung Memorial Hospital, Kaohsiung, Taiwan; <sup>2</sup>Graduate Institute of Medicine, Kaohsiung Medical University, Kaohsiung, Taiwan; <sup>3</sup>Department of Medicine, University of Arizona, Tucson, Arizona, USA and <sup>4</sup>Department of Anesthesiology, Chang-Gung Memorial Hospital, Kaohsiung, Taiwan

Diabetes is associated with renal calcium and magnesium wasting, but the molecular mechanisms of these defects are unknown. We measured renal calcium and magnesium handling and investigated the effects of diabetes on calcium and magnesium transporters in the thick ascending limb and distal convoluted tubule in streptozotocin (STZ)-induced diabetic rats. Rats were killed 2 weeks after inducing diabetes, gene expression of calcium and magnesium transporters in the kidney was determined by real-time polymerase chain reaction, and the abundance of protein was assessed by immunoblotting. Our results showed that diabetic rats had significant increase in the fractional excretion for calcium and magnesium (both  $P < 0.01$ ), but not for sodium. Reverse transcriptase-polymerase chain reaction revealed significant increases in messenger RNA abundance of transient potential receptor (TRP) V5 ( $223 \pm 10\%$ ), TRPV6 ( $177 \pm 9\%$ ), calbindin-D28k ( $231 \pm 8\%$ ), and TRPM6 ( $165 \pm 8\%$ ) in diabetic rats. Sodium chloride cotransporter was also increased ( $207 \pm 10\%$ ). No change was found in paracellin-1 (cortex:  $108 \pm 8\%$ ; medulla:  $110 \pm 10\%$ ). Immunofluorescent studies of renal sections showed significant increase in calbindin-D28k ( $238 \pm 10\%$ ) and TRPV5 ( $211 \pm 10\%$ ), but no changes in paracellin-1 in Western blotting (cortex:  $110 \pm 7\%$ ; medulla:  $99 \pm 7\%$ ). Insulin administration completely corrected the hyperglycemia-associated hypercalciuria and hypermagnesiuria, and reversed the increase of calcium and magnesium transporter abundance. In conclusion, our results demonstrated increased renal calcium and magnesium transporter abundance in STZ-induced diabetic rats, which may represent a compensatory adaptation for the increased load of calcium and magnesium to the distal tubule.

*Kidney International* (2006) **69**, 1786–1791. doi:10.1038/sj.ki.5000344; published online 22 March 2006

**Correspondence:** H-C Chen, Division of Nephrology, Department of Medicine, Graduate Institute of Medicine, Kaohsiung Medical University, 100 Tz-You 1st Road, Kaohsiung, 807 Taiwan. E-mail: [chenhc@kmu.edu.tw](mailto:chenhc@kmu.edu.tw)

Received 11 May 2005; revised 8 December 2005; accepted 14 December 2005; published online 22 March 2006

**KEYWORDS:** diabetes mellitus; hypercalciuria; hypermagnesiuria; TRPV5; TRPM6; paracellin-1

It is well known that carbohydrate intake is associated with increased renal calcium excretion.<sup>1</sup> Furthermore, glucose ingestion can augment both renal calcium and magnesium excretion.<sup>2</sup> Hypercalciuria is an early finding of uncontrolled diabetes mellitus (DM) in humans and experimental animals.<sup>3,4</sup> The effect of DM on calcium metabolism is complex, but essentially it is associated with a negative calcium balance hallmarked by both bone and renal loss.<sup>3–5</sup> The underlying mechanism contributing to diabetes-associated renal calcium loss has been investigated extensively. In addition to osmotic effect, a specific tubular defect in calcium reabsorption, which leads to calcium loss, has been proposed.<sup>6–8</sup> Though most ultrafiltered calcium is reabsorbed in the proximal tubules,<sup>9</sup> previous microperfusion studies did not reveal any decrease of calcium reabsorption in this segment in diabetic animals.<sup>6–8</sup> In fact, two sites have been identified as having defect in calcium transport: the thick ascending limb (TAL) of Henle's loop and terminal nephron.<sup>6</sup>

Hypomagnesemia is a common complication of uncontrolled DM.<sup>10,11</sup> Among factors contributing to hypomagnesemia, renal magnesium loss is the major determinant.<sup>11</sup> Similar to calcium, renal magnesium wasting is probably because of defects in the TAL, where more than 50% of ultrafiltered magnesium is reabsorbed.<sup>12</sup> This is supported by the finding that insulin stimulates magnesium transport in microperfused mouse TAL.<sup>13</sup> Intriguingly, the tubular defect observed in diabetes does not affect all solutes equally. Although glycosuria causes diuresis and natriuresis, urinary excretion of calcium and magnesium is much greater than that of other solutes.<sup>4</sup> Therefore, it is likely that specific calcium and magnesium transport molecules may be involved in renal wasting of these minerals.

Recently, several calcium and magnesium transport molecules were identified and specifically located in the TAL or distal convoluted tubule (DCT).<sup>14–16</sup> Paracellin-1, also named as claudin-16 and as a member of claudin family, has

been identified in the TAL and is responsible for paracellular transport of calcium and magnesium.<sup>16</sup> Dysfunction of the paracellin-1 gene causes congenital hypomagnesemia with hypercalciuria.<sup>17</sup> In the DCT, transient potential receptor (TRP) V5 and TRPV6 have been identified as calcium channels, which finely tune the final urinary calcium concentration.<sup>18</sup> Another member of the TRP family, TRPM6, is expressed in kidneys and intestines and is responsible for transcellular magnesium absorption in the DCT.<sup>19</sup> Whether these transport molecules are involved in the pathogenesis of diabetes-induced renal calcium and magnesium wasting has not been studied. By investigating the effects of diabetes on these molecules, we hope to explore the molecular mechanisms involved in diabetes-associated tubular defects in calcium and magnesium transports.

## RESULTS

Diabetic rats had a 4–5-fold increase in daily urine output compared to the control rats ( $P < 0.01$ , Table 1). With insulin treatment, which effectively reduced blood glucose levels, the urinary output was normalized. There was no difference in serum creatinine, sodium, calcium, magnesium, or phosphorous levels among the three groups. Venous blood pH value was also similar among the three groups (pH, control:  $7.41 \pm 0.09$ ; diabetic:  $7.42 \pm 0.03$ ; diabetics with insulin treatment:  $7.40 \pm 0.06$ ,  $P > 0.05$ ).

The calculated creatinine clearance was not different between diabetic and control rats (Table 1). Daily urinary excretion of sodium, calcium, and magnesium was markedly increased in diabetic rats compared to that of the control group. A two-fold increase in sodium excretion was found in the diabetic group, whereas there was an eight-fold increase in calcium and five-fold increase in magnesium excretion (sodium:  $1.72 \pm 0.18$  vs  $0.86 \pm 0.06$  mmol/day/100 g; calcium:  $2.81 \pm 0.43$  vs  $0.38 \pm 0.05$  mg/day/100 g; magnesium:  $3.82 \pm 0.38$  vs  $0.77 \pm 0.15$  mg/day/100 g, all  $P < 0.01$ , Figure 1). In the insulin-treated group, none of these incremental changes in sodium, calcium, or magnesium were observed ( $P > 0.05$ ).

The fractional excretion of sodium did not change significantly in diabetic group ( $0.78 \pm 0.09$  vs  $0.58 \pm 0.07\%$ ,  $P > 0.05$ , Figure 2a). There was significant increase in fraction excretion of calcium and magnesium (Ca:  $3.59 \pm 0.58$  vs

$0.56 \pm 0.08\%$ ; Mg:  $19.18 \pm 1.51$  vs  $4.95 \pm 1.56\%$ , both  $P < 0.01$ , Figure 2b and c). Insulin treatment not only reduced the blood glucose level, but also reduced fraction excretion of calcium and magnesium. As balance studies were not performed, the increased daily urinary excretion, or fractional excretion of calcium and magnesium, may be because of increased intake of calcium and magnesium, increased renal excretion of calcium and magnesium, or the combination of the two. Nevertheless, these results suggest that filtered load of calcium and magnesium was increased in diabetic rats.

## Messenger RNA expression

In diabetic rats, there was upregulation of TRPV5, TRPV6, and calbindin-D28K genes compared to normal animals (TRPV5:  $223 \pm 10\%$ , TRPV6:  $177 \pm 9\%$ , calbindin-D28k:  $231 \pm 8\%$ , all  $P < 0.05$ , Figure 3). The sodium chloride cotransporter gene expression also increased significantly ( $207 \pm 10\%$ ,  $P < 0.05$ ). In the insulin-treated diabetic group, no changes were found in gene expression (TRPV5:  $108 \pm 7\%$ , TRPV6:  $102 \pm 8\%$ , calbindin-D28k:  $98 \pm 9\%$ , sodium chloride cotransporter:  $108 \pm 12\%$ , all  $P > 0.05$ ). Increased expression was also noted in TRPM6 in diabetic rats ( $165 \pm 8\%$ ,  $P < 0.05$ ), but not in the insulin-treated

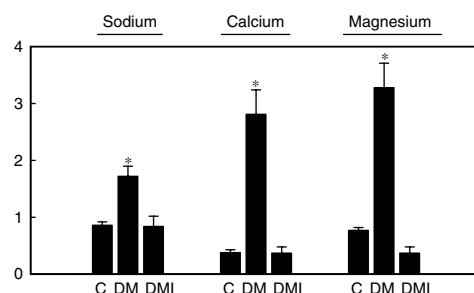


**Figure 1** | Daily urinary excretion of sodium (mmol/24 h/100 g), calcium (mg/24 h/100 g), and magnesium (mg/24 h/100 g) in three groups of rats: control (C), DM, and DMI. \* $P < 0.01$  compared to the controls.

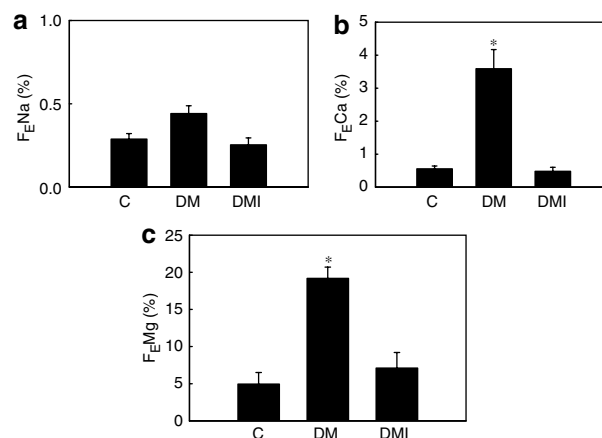


**Figure 2** | Fractional excretion ( $F_E$ , %) of (a) sodium, (b) calcium, and (c) magnesium in the three groups of rats: control (C), DM, and DMI. \* $P < 0.01$  compared to the controls.

**Table 1** | Biochemical data of three groups of animals

	Control	Diabetes	Diabetes-insulin treated
Body weight (g)	311.7 ± 5.9	325.9 ± 12.3	290.2 ± 8.6
Serum glucose (mg/dl)	105.4 ± 6.3	441.6 ± 26.5*	141.3 ± 34.6
Serum Na (mmol/l)	138 ± 3.3	136 ± 2.9	137 ± 3.1
Serum Cr (mg/dl)	0.35 ± 0.02	0.49 ± 0.03	0.43 ± 0.02
Serum Ca (mg/dl)	9.8 ± 0.1	9.5 ± 0.2	10.2 ± 0.1
Serum Mg (mg/dl)	1.9 ± 0.2	1.9 ± 0.1	1.8 ± 0.1
Serum Pi (mg/dl)	7.9 ± 0.6	7.8 ± 0.9	7.6 ± 1.0
Urine volume (ml/day)	40.0 ± 2.6	133.9 ± 14.5*	34.0 ± 10.0
Creatinine clearance (ml/24 h)	2.7 ± 0.1	2.9 ± 0.4	2.4 ± 0.1

\* $P < 0.05$ , diabetes vs control.

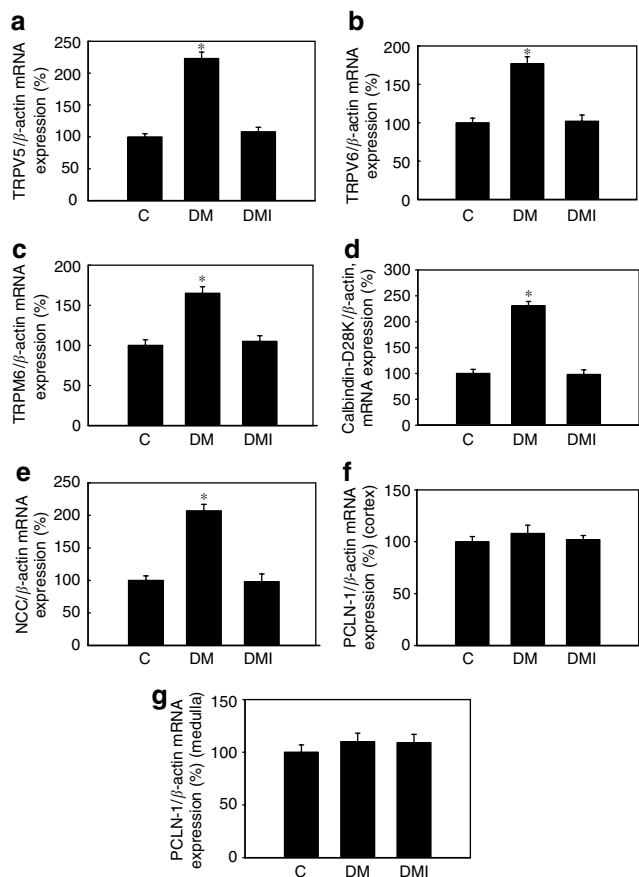


**Figure 3 | Gene expression of (a) TRPV5, (b) TRPV6, (c) TRPM6, (d) calbindin-D28k, (e) sodium chloride cotransporter (NCC), and (f) cortex; (g) medulla) paracellin-1 (PCLN-1) among the three groups of rats: control (C), DM, and DMI. We used  $\beta$ -actin as the reference gene. \* $P < 0.05$  compared to the controls.**

diabetic group ( $105 \pm 8\%$ ,  $P > 0.05$ ). As the paracellin-1 is expressed in the thick ascending limb of Henle, which extends from the medulla to cortex, gene expression of paracellin-1 was examined in both renal section tissues. Paracellin-1 showed no change in the diabetic and insulin-treated diabetic groups (cortex: diabetic:  $108 \pm 8\%$ , insulin-treated diabetic:  $102 \pm 4\%$ , both  $P > 0.05$ ; medulla: diabetic:  $110 \pm 10\%$ , insulin-treated diabetic:  $109 \pm 8\%$ ,  $P > 0.05$ ).

#### Immunoblotting and immunofluorescent studies

To examine whether the effects on messenger RNA (mRNA) expression were translated into the protein level, Western blotting was performed. The abundance of calbindin-D28k protein was increased significantly in diabetic rats compared to the control group. This increase was not found in the insulin-treated group (diabetic:  $198 \pm 8\%$ , insulin-treated diabetic:  $105 \pm 9\%$ , Figure 4a). The study on protein abundance of paracellin-1 did not show any significant alternations both in the cortex and medulla (cortex: diabetic:  $110 \pm 7\%$ , insulin-treated diabetic:  $98 \pm 6\%$ , Figure 4b; medulla: diabetic:  $99 \pm 7\%$ , insulin-treated diabetic:  $95 \pm 8\%$ , Figure 4c). The immunofluorescent staining study revealed that there was significant increase in protein

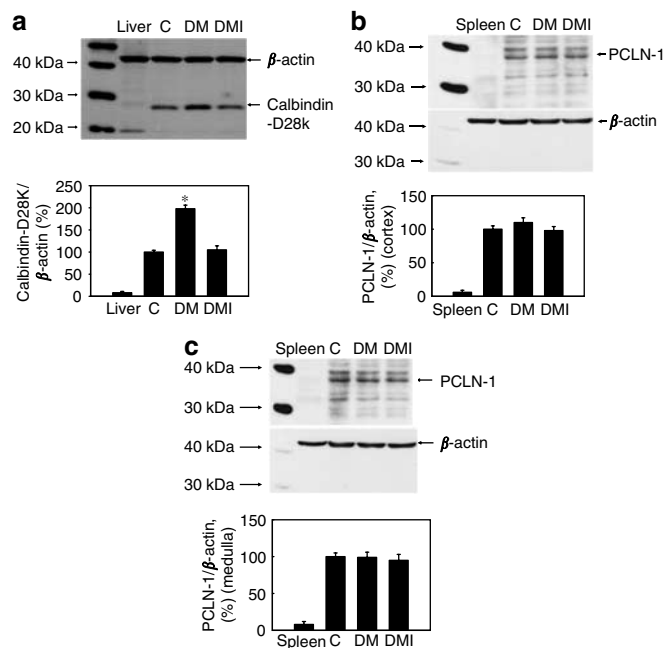


**Figure 4 | Immunoblotting results for (a) calbindin-D28k and (b) cortex; (c) medulla) paracellin-1 for the three groups of animals: control (C), DM, and DMI. Liver or spleen tissue was selected as a negative control. The band of PCLN-1 was indicated by an arrow based on its molecular weight of 35 kDa. \* $P < 0.05$  compared to the controls.**

expression of calbindin-D28k in diabetic rats and no change in insulin-treated diabetics (diabetic:  $238 \pm 10\%$ , insulin-treated:  $118 \pm 7\%$ , Figure 5a). The increased protein expression was also observed in TRPV5 (diabetic:  $211 \pm 10\%$ , insulin-treated:  $108 \pm 8\%$ , Figure 5b).

#### DISCUSSION

Our results demonstrated that increased urinary calcium and magnesium content in untreated DM is associated with increased abundance of TRPV5, TRPV6, TRPM6, and calbindin-D28k in the kidney. These physiological changes and changes in gene expression are reversed by insulin treatment. We did not find any significant changes in paracellin mRNA or protein abundance in diabetic kidneys.

The TRPV5 is exclusively expressed in DCT and regarded as a gate keeper for calcium entry in DCT.<sup>20</sup> TRPV6 is expressed in the DCT and the terminal nephron,<sup>21</sup> but the role of TRPV6 in renal calcium reabsorption is still controversial in the literature. The TRPV5 knockout mice demonstrated marked renal calcium wasting and reduced bone mass.<sup>22</sup> These findings suggest that renal TRPV6 is not capable of compensating for the absence of TRPV5, or alternatively TRPV6 in the DCT is dependent on TRPV5. Calbindin-D28k is one of the important intracellular calcium-binding proteins,<sup>23</sup> and is expressed in DCT, connecting tubule, and collecting duct in rat kidney.<sup>24</sup> In addition to facilitating intracellular calcium transport, calbindin-D28k also acts as a buffer to avoid rapid increase in intracellular calcium concentration, which leads to cell

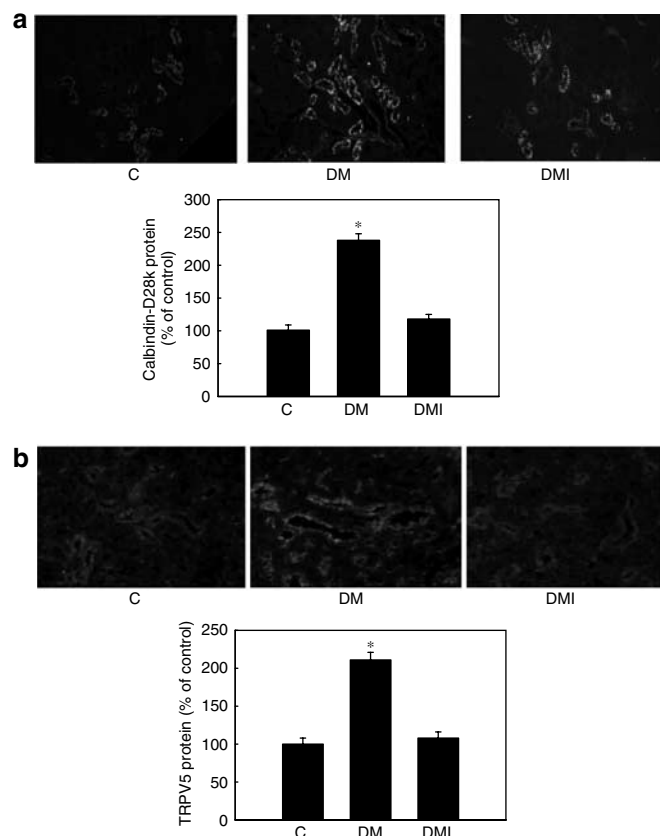


**Figure 5 | Immunofluorescent results for (a, original magnification  $\times 100$ ) calbindin-D28k and (b, original magnification  $\times 100$ ) TRPV5 for the three groups of animals: control (C), DM, and DMI. \* $P < 0.05$  compared to the controls.**

toxicity.<sup>25,26</sup> The lack of calbindin-D28k is associated with significant renal calcium leak.<sup>27</sup> Our findings of upregulation of renal calbindin-D28k in diabetes is consistent with a previous report, which demonstrated that renal calbindin-D28k mRNA abundance increased 2–3-fold up to day 18 in diabetic pregnant rats when compared to non-diabetic pregnant rats.<sup>28</sup> More recently, another study showed that renal calbindin-D28k protein in diabetic rats was not different from that in control rats.<sup>29</sup> In this study, crude membrane preparation from the kidney was used. As calbindin-D28k is a cytosolic protein, it is possible that the amount of calbindin-D28k was underestimated in the previous study.

The simultaneous increase in abundance of TRPV5, TRPV6, and calbindin-D28k in diabetes-associated hypercalciuria suggests a coordinated response to increased calcium load in urinary flow. Previous study on regulation of renal epithelial calcium channel shows that calcium load is an important factor regulating the expression of the apical calcium channel.<sup>30</sup> Interestingly, TRPV5, TRPV6, and calbindin-D28k are known to be regulated by vitamin D. In uncontrolled diabetes, the  $1, 25$  (OH)<sub>2</sub> vitamin D<sub>3</sub> level is significantly reduced.<sup>29</sup> It appears that in diabetic kidney, the effect of calcium load may override the effect of vitamin D on gene regulation of apical calcium channels and calcium-binding protein.

In our study, although serum magnesium levels were not decreased in diabetic rats for the 2-week duration, we were able to demonstrate the upregulation of the TRPM6 gene in diabetes-associated renal magnesium loss. Hypomagnesemia may become evident with longer experimental durations. The TRPM6 has been recognized as an important molecule participating in intestinal and renal magnesium absorption. In the kidney, the expression of TRPM6 is confined to the DCT and colocalized with calbindin-D28k.<sup>19</sup> More recently, inhibition of TRPM6 was found as the etiology of Tacrolimus (FK506)-related renal magnesium loss with resulting hypomagnesemia.<sup>31</sup> In diabetes, the upregulation of TRPM6 may be similar to that in TRPV5 and TRPV6 as a compensatory mechanism to increased solute load. Similar compensatory upregulation of transporters for sodium and water has been reported previously.<sup>32</sup> The sodium chloride cotransporter, which is exclusively expressed in the DCT, also displayed upregulation in our experiment. This result was consistent with those of other studies.<sup>29,33</sup> In addition, sodium-potassium-chloride cotransporter in the thin ascending limb of Henle, epithelial sodium channel in the connecting tubule and collecting duct, and water channels, aquaporins in collecting duct, all showed a compensatory increase in diabetic animals to avoid excessive sodium or water loss.<sup>33,34</sup>

The TAL plays an important role in renal calcium and magnesium reabsorption, primarily via the paracellular transport.<sup>35,36</sup> The reabsorption of calcium and magnesium in TAL is a passive process, which is voltage- and load-dependent. We did not find any significant changes in both mRNA expression and protein abundance of paracellin-1 in diabetic kidneys. As mentioned earlier, previous micropuncture and micropfusion studies demonstrated calcium reabsorption defect in the TAL in diabetic animals.<sup>6–8</sup> Our study has ruled out changes in paracellin-1 gene expression as a possible cause of diabetes-associated TAL defect in renal calcium and magnesium reabsorption. As insulin is known to increase transepithelial potential difference (Vt) in TAL,<sup>13</sup> it is possible that the lack of insulin in diabetes may reduce Vt, thus suppressing calcium and magnesium reabsorption. The exact mechanism remains to be determined.

Adequate control of plasma glucose by insulin treatment effectively reversed renal calcium and magnesium loss in our study. This effect is accompanied by normalization of increased calcium and magnesium transporter abundance. Previous experiments showed that a 2-week delay of insulin administration failed to reverse renal calcium loss in diabetic animals. It was proposed that an irreversible tubular defect might develop if diabetes is left untreated.<sup>37</sup> Therefore, strict and early glucose control is critical for preventing diabetes-related disturbance in mineral metabolism.

In conclusion, our study is the first to demonstrate the increased abundance of calcium and magnesium transport molecules and binding protein in the DCT in experimentally induced diabetes. It is likely that there is a common compensatory mechanism shared by transporters for many solutes in the diabetic kidney. In our study, diabetes does not



affect the abundance of paracellin-1 in the kidney. The mechanism of increased renal calcium and magnesium excretion in the TAL remains unclear. Correction of hyperglycemia with insulin not only reduces renal calcium and magnesium excretion but also reverses the changes in gene expression.

## MATERIALS AND METHODS

### Animals

Male Sprague–Dawley rats weighing 250–350 g were used for this experiment. All rats were maintained under a constant 12-h photoperiod at temperatures between 21 and 23°C. They were allowed free access to food and water. The food contained sodium (0.33%), calcium (1.0%), and magnesium (0.16%). The animals were divided into three groups: diabetic rats, control rats, and insulin-treated diabetic rats.

### Diabetic rats

Rats ( $n = 12$ ) were rendered diabetic by streptozotocin (STZ, Sigma, St Louis, MO, USA) at the dosage of 65 mg/kg via a single intraperitoneal injection. STZ was freshly dissolved in citrate buffer (pH 4.8) and maintained on ice until injection. Diabetes was confirmed by the development of glycemia ( $\geq 300$  mg/dl glucose) 24 h after injection. As diabetic rats developed polyuria from hyperglycemia, they were allowed to eat and drink *ad lib* in order to avoid volume depletion, which is known to affect renal calcium and magnesium reabsorption.

### Control rats

Control rats ( $n = 10$ ) received a citrate buffer injection alone. Blood glucose levels were determined when the rats were killed.

### Insulin-treated diabetic rats

Six rats were induced diabetic with STZ, and then received insulin therapy (Ultratard HM, Novo Nordisk, Bagsvaerd, Denmark) via subcutaneous injection daily for 2 weeks until they were killed. The insulin dosage was adjusted daily to maintain blood glucose level in the range of 100–200 mg/dl.

### Biochemical studies

Urine samples (24-h) were collected from all the three groups of animals using individualized metabolic cages. The rats were then harvested and blood samples were used for biochemical measurements. Serum and urinary creatinine, sodium, calcium, and magnesium were measured. The levels of creatinine, sodium, calcium, magnesium, and phosphorous were determined using the SYNCHRON CX DELTA system (Beckman, Fullerton, CA, USA) by various methods according to manufacturer's operating protocol. Then, 24 h urinary excretion of sodium, calcium, and magnesium was calculated and presented as mg per 100 g of body weight. The fractional excretion ( $F_E$ ) of sodium, calcium, and magnesium was calculated by the standard method. Venous blood samples were sent for blood gas analysis of each group of animals to evaluate their acid–base status.

### Molecular studies

**RNA isolation and complementary DNA synthesis.** Renal cortex and medulla were dissected and total RNA was isolated from each section using TRIzol reagent (Invitrogen, Carlsbad, CA, USA). Reverse transcription for complementary DNA synthesis was

performed using the reverse transcription system (Promega, Madison, WI, USA).

### Real-time polymerase chain reaction

The alternations in gene expression were quantified utilizing real-time polymerase chain reaction. The emission signal was assessed using the fluorescent dye SYBR Green (ABI, Foster city, CA, USA). The molecules involved in calcium transport, including TRPV5, TRPV6, and calbindin-D28k, were assessed in all three animal groups. Gene expression of sodium chloride cotransporter was also investigated. For magnesium transport, the TRPM6 and paracellin-1 genes were studied. The mRNA abundance of  $\beta$ -actin was used as the internal reference for each gene evaluated. The synthesized complementary DNA was then subjected to real-time polymerase chain reaction using the ABI prism 7900 HT Sequence Detection System (ABI, Foster City, CA, USA). The primer sequences of the studied genes are listed in Table 2. To determine the gene expression, genes investigated in the present study were calculated as  $2^{-(\beta\text{-actin } Ct - \text{target gene } Ct)}$ , where  $Ct$  represents the first cycle at which the output signal exceeds the threshold signal.<sup>38</sup> Polymerase chain reaction of each gene was performed in triplicate to obtain a mean value.<sup>39</sup> The changes in gene expression are presented as percentages of control animal values.

### Immunoblotting study

Renal cortical and medullary sections were frozen at  $-80^\circ\text{C}$  and then homogenized at  $4^\circ\text{C}$  in protein lysis buffer solution containing 20 mM Tris-HCl (pH 7.4), 0.1% sodium dodecyl sulfate, 5-mM ethylenediamine tetraacetate, 1% Triton X-100, and a protease inhibitor cocktail tablet (Roche, Penzberg, Germany). After centrifugation at 12 000 g for 10 min at  $4^\circ\text{C}$ , the protein concentrations were determined using bicinchoninic acid protein assays. The protein samples were then run on 10% sodium dodecyl sulfate-polyacrylamide gel electrophoresis for calbindin-D28k and paracellin-1, and were then transferred to nitrocellulose membranes.  $\beta$ -Actin was used as the internal control in this study. After blocking with 10% non-fat milk, the membrane was incubated with goat anti-mouse calbindin-D28k monoclonal antibody (1:5000, Sigma) for 16 h. Further washing in 5% blocking milk was performed and the membrane was incubated with goat anti-rabbit antibody conjugated with horseradish peroxidase (1:30 000) for 3 min. Rabbit anti-human paracellin-1 monoclonal antibody (1:500, Alpha Diagnostics International, San Antonio, TX, USA) was used as primary antibody for paracellin-1 detection, with incubation for 16 h. The abundance of studied protein was then quantified by densitometric analyses. The changes in protein abundance are presented as percentages of control animal values.

**Table 2 | Lists of primers used for real-time PCR**

Gene	Forward primer	Reverse primer
$\beta$ -actin	agtacccattgaacacggc	ttttcacggttgcccttagg
CBD28K	ggagctgcagaacttgatcc	gcagcaggaaattctctcg
NCC	gaacggcacaccattgtaga	gccttgactcccactccat
TRPV5	tgttaccgccccctcaag	cacagcccaatgactgtca
TRPV6	atccggcgtatgcaca	agttttctctgagtcttttcca
TRPM6	aaagcatgaggtatcagc	cttcacaatgaaacctgccc
PCLN-1	cagatgcgagtgccctgta	agcaccgcaagagagtgaga

CBD28K, calbindin-D28k; NCC, sodium chloride cotransporter; PCLN-1, paracellin-1; TRPV5, TRPV6 and TRPM6, transient receptor potential V5, V6, and M6.

### Immunofluorescence microscopy

Paraffin-embedded kidney cortex tissue was used for calbindin-D28k and TRPV5 protein assessment in three groups of animals. Sections of 5  $\mu\text{m}$  thickness were fixed with 4% paraformaldehyde for 15 min and incubated with primary antibody (goat anti-mouse calbindin-D28k monoclonal antibody 1:500, Sigma, and rabbit anti-rat ECaC1 1:100, Alpha Diagnostic International, San Antonio, TX, USA) for 16 h, and then with fluorescein isothiocyanate-conjugated secondary antibodies for calbindin-D28k (Jackson ImmunoResearch Laboratories, Inc., West Grove, PA, USA), and streptavidin/fluorescein isothiocyanate-conjugated secondary antibody for TRPV5 (DakoCytomation, Dako Corporation, Carpinteria, CA, USA) for 30 min. The immunofluorescence pictures were then taken using a Zeiss fluorescence microscope connected with a digital photo camera (Evolution VF, MediaCybernetics, Silver Spring, MD, USA). Semi-quantitative determination of the protein expression was performed with the Image-Pro Plus 5.0 image analysis software. Amount of protein was expressed as the mean of integrated optical density. The alternation is expressed as percentage of control animal value.<sup>39</sup>

### Statistical analyses

Data are presented as means  $\pm$  s.e.m. Statistical analyses of the data were performed using SPSS-PC software. Unpaired Student's *t*-tests were used to compare differences between two groups. To determine the significant difference among controls, diabetic, and insulin-treated diabetic rats, one-way analysis of variance and Tukey's test were used. A *P*-value of  $<0.05$  was considered statistically significant for all tests.

### ACKNOWLEDGMENTS

This work was supported by a grant from the National Science Council of the Republic of China (NSC94-2314-B-182A-119), and a grant from Dialysis Clinic Inc., a non-profit organization to YHL. Part of this work has been presented at the American Society of Nephrology, 2004, St Louis, MO, USA.

### REFERENCES

- Lemann Jr J, Piering WF, Lennon EJ. Possible role of carbohydrate-induced calciuria in calcium oxalate kidney-stone formation. *N Engl J Med* 1969; **280**: 232–237.
- Lemann Jr J, Lennon EJ, Piering WR et al. Evidence that glucose ingestion inhibits net renal tubular reabsorption of calcium and magnesium in man. *J Lab Clin Med* 1970; **75**: 578–585.
- Raskin P, Stevenson MR, Barilla DE, Pak CY. The hypercalciuria of diabetes mellitus: its amelioration with insulin. *Clin Endocrinol* 1978; **9**: 329–335.
- Anwana AB, Garland HO. Renal calcium and magnesium handling in experimental diabetes mellitus in the rat. *Acta Endocrinol (Copenh)* 1990; **122**: 479–486.
- Shires R, Teitelbaum SL, Bergfeld MA et al. The effect of streptozotocin-induced chronic diabetes mellitus on bone and mineral homeostasis in the rat. *J Lab Clin Med* 1981; **97**: 231–240.
- Guruprakash GH, Krothapalli RK, Rouse D et al. The mechanism of hypercalciuria in streptozotocin-induced diabetic rats. *Metabolism* 1988; **37**: 306–311.
- Garland HO, Harris PJ, Morgan TO. Calcium transport in the proximal convoluted tubule and loop of Henle of rats made diabetic with streptozotocin. *J Endocrinol* 1991; **131**: 373–380.
- Boland PS, Garland HO. Renal micropuncture study of the effects of  $\alpha$ -glucose tubular calcium handling in the anaesthetized rat. *Exp Physiol* 1993; **78**: 175–181.
- Friedman PA, Gesek FA. Cellular calcium transport in renal epithelia: measurement, mechanisms and regulation. *Physiol Rev* 1995; **75**: 429–471.
- McNair P, Christensen MS, Christiansen C et al. Renal hypomagnesaemia in human diabetes mellitus: its relation to glucose homeostasis. *Eur J Clin Invest* 1982; **12**: 81–85.
- Tosiello L. Hypomagnesaemia and diabetes mellitus. A review of clinical implications. *Arch Intern Med* 1996; **156**: 1143–1148.
- Garland HO. New experimental data on the relationship between diabetes mellitus and magnesium. *Magn Res* 1992; **5**: 193–202.
- Mandon B, Siga E, Chabardes D et al. Insulin stimulates  $\text{Na}^+$ ,  $\text{Cl}^-$ ,  $\text{Ca}^{2+}$  and  $\text{Mg}^{2+}$  transports in TAL of mouse nephron: cross-potential with AVP. *Am J Physiol* 1993; **265**: F361–F369.
- Hoenderop JG, van der Kemp AW, Hartog A et al. Molecular identification of the apical  $\text{Ca}^{2+}$  channel in 1, 25-dihydroxyvitamin D3-responsive epithelia. *J Biol Chem* 1999; **274**: 8375–8378.
- Peng JB, Chen XZ, Berger UV et al. Molecular cloning and characterization of a channel-like transporter mediating intestinal calcium absorption. *J Biol Chem* 1999; **274**: 22739–22746.
- Simon DB, Lu Y, Choate KA et al. Paracellin-1, a renal tight junction protein required for paracellular  $\text{Mg}^{2+}$  resorption. *Science* 1999; **285**: 103–106.
- Blanchard A, Jeunemaitre X, Coudol P et al. Paracellin-1 is critical for magnesium and calcium reabsorption in the human thick ascending limb of Henle. *Kidney Int* 2001; **59**: 2206–2215.
- den Dekker E, Hoenderop JG, Nilius B, Bindels RJ. The epithelial calcium channels, TRPV5 & TRPV6: from identification towards regulation. *Cell Calcium* 2003; **33**: 497–507.
- Voets T, Nilius B, Hoefs S et al. TRPM6 forms the  $\text{Mg}^{2+}$  influx channel involved in intestinal and renal  $\text{Mg}^{2+}$  absorption. *J Biol Chem* 2004; **279**: 19–25.
- Hoenderop JG, Nilius B, Bindels RJ. ECaC: the gatekeeper of transepithelial  $\text{Ca}^{2+}$  transport. *Biochim Biophys Acta* 2002; **1600**: 6–11.
- Nijenhuis T, Hoenderop JG, van der Kemp AW, Bindels RJ. Localization and regulation of the epithelial  $\text{Ca}^{2+}$  channel TRPV6 in the kidney. *J Am Soc Nephrol* 2003; **14**: 2731–2740.
- Hoenderop JG, van Leeuwen JP, van der Eerden BC et al. Renal  $\text{Ca}^{2+}$  wasting, hyperabsorption, and reduced bone thickness in mice lacking TRPV5. *J Clin Invest* 2003; **112**: 1906–1914.
- Christakos S, Gabrielides C, Rhoten WB. Vitamin D-dependent calcium binding proteins: chemistry, distribution, functional considerations, and molecular biology. *Endocr Rev* 1989; **10**: 3–26.
- Taylor AN, McIntosh JE, Bourdeau JE. Immunocytochemical localization of vitamin D-dependent calcium-binding protein in renal tubules of rabbit, rat, and chick. *Kidney Int* 1982; **21**: 765–773.
- Wu MJ, Lai LW, Lien YH. Cytoprotective effects of calbindin-D<sub>28k</sub> against antimycin-A induced hypoxic injury in proximal tubular cells. *Life Sci* 2002; **71**: 559–569.
- Wu MJ, Lai LW, Lien YH. Effect of calbindin-D<sub>28k</sub> on cyclosporine toxicity in cultured renal proximal tubular cells. *J Cell Physiol* 2004; **200**: 395–399.
- Lee CT, Huynh VM, Lai LW, Lien YH. Cyclosporine A-induced hypercalciuria in calbindin-D28k knockout and wild-type mice. *Kidney Int* 2002; **62**: 2055–2061.
- Hamilton K, Tein M, Glazier J et al. Altered calbindin mRNA expression and calcium regulating hormones in rat diabetic pregnancy. *J Endocrinol* 2000; **164**: 67–76.
- Ward RT, Yau SK, Mee AP et al. Functional, molecular, and biochemical characterization of streptozotocin-induced diabetes. *J Am Soc Nephrol* 2001; **12**: 779–790.
- Peng JB, Brown EM, Hediger MA. Apical entry channels in calcium-transporting epithelia. *News Physiol Sci* 2003; **18**: 158–163.
- Nijenhuis T, Hoenderop JG, Bindels RJ. Downregulation of Ca (2+) and Mg (2+) transport proteins in the kidney explains tacrolimus (FK506)-induced hypercalciuria and hypomagnesaemia. *J Am Soc Nephrol* 2004; **15**: 549–557.
- Kim D, Sands JM, Klein JD. Changes in renal medullary transport proteins during uncontrolled diabetes mellitus in rats. *Am J Physiol Renal Physiol* 2003; **285**: F303–F309.
- Song J, Knepper MA, Verbalis JG, Ecelbarger CA. Increased renal ENaC subunit and sodium transporter abundances in streptozotocin-induced type 1 diabetes. *Am J Physiol Renal Physiol* 2003; **285**: F1125–F1137.
- Nejsum LN, Kwon TH, Marples D et al. Compensatory increase in AQP2, p-AQP2, and AQP3 expression in rats with diabetes mellitus. *Am J Physiol Renal Physiol* 2001; **280**: F715–F726.
- Quamme GA. Renal magnesium handling: new insights in understanding old problems. *Kidney Int* 1997; **52**: 1180–1195.
- Friedman PA. Mechanisms of renal calcium transport. *Exp Nephrol* 2000; **8**: 343–350.
- Hoskins B, Scott JM. Evidence for a direct action of insulin to increase renal reabsorption of calcium and for an irreversible defect in renal ability to conserve calcium due to prolonged absence of insulin. *Diabetes* 1984; **33**: 991–994.
- Pfaffi MW. A new mathematical model for relative quantification in real-time RT-PCR. *Nucleic Acids Res* 2001; **29**: 2002–2007.
- Lee CT, Shang S, Lai LW et al. Effect of thiazide on renal gene expression of apical calcium channels and calbindins. *Am J Physiol Renal Physiol* 2004; **276**: F1164–F1170.